IEEE Access
Multidisciplinary | Rapid Review | Open Access Journal

Received August 25, 2017, accepted October 1, 2017, date of publication October 10, 2017, date of current version February 1, 2018.

Digital Object Identifier 10.1109/ACCESS.2017.2761788

The Modeling and Cross-Layer Optimization of 802.11p VANET Unicast

YU XIE[1], IVAN WANG-HEI HO[1,2], Member, IEEE, AND ELMER R. MAGSINO[1]

[1]Department of Electronic and Information Engineering, The Hong Kong Polytechnic University, Hong Kong
[2]Research Institute for Sustainable Urban Development, The Hong Kong Polytechnic University, Hong Kong

Corresponding author: Ivan Wang-Hei Ho (ivanwh.ho@polyu.edu.hk)

The work of I. W.-H. Ho and E. R. Magsino was supported in part by the Early Career Scheme under Project 25200714 established under the University Grant Committee of the Hong Kong Special Administrative Region, China, and in part by The Hong Kong Polytechnic University under Project G-YBK6, Project G-YBR2, and Project 4-ZZCZ. The work of Y. Xie was supported by the National Natural Science Foundation of China under Project 61401384.

ABSTRACT Vehicular ad-hoc networks (VANETs) play an important role in enabling ubiquitous communications and connectivity among vehicles in intelligent transportation systems. Various messages can be transmitted in a VANET to improve road safety and furnish multiple types of application services. Therefore, the evaluation of VANET performance and its optimization should be considered. Previous conventional considerations regarding VANET modeling merely incorporated a general homogeneous road traffic scenario. Furthermore, prior research works primarily focused on the broadcasting performance in VANETs, since the safety beacon packets are transmitted in periodic broadcast. However, the exchange of some important data between vehicles is better accomplished by using unicast instead of broadcast with the retransmission mechanism. On the other hand, in the context of VANET optimization, most conventional schemes required continuous monitoring of the network by measuring the number of neighboring nodes to configure the transmission power or adjusting the transmission rate accordingly. Such constant tracking leads to large transmission overheads and measurement delay. In this paper, we propose a set of 802.11p unicast modeling and optimization methodologies to determine the optimal network parameters without continuously monitoring the vehicles in vicinity. This is accomplished by integrating a stochastic urban traffic model in the analysis then performing a cross-layer optimization for each network node to reduce packet collisions. The optimal transmission range and contention window size at different locations are derived based on the spatio-temporal velocity profile and are made known to entering vehicles. These aid the vehicles to configure their transmission power and rate accordingly upon entering a road segment. We evaluate the proposed system in terms of the network delay and throughput performance. Considerable simulation runs to verify the feasibility of the proposed model and optimization methods. Our results indicate that delay (throughput) is improved by about 53% (120%) on average for homogeneous traffic and 45% (104%) on average for heterogeneous traffic.

INDEX TERMS Unicast performance modeling, cross-layer optimization, stochastic traffic modeling, vehicular ad hoc network (VANET).

I. INTRODUCTION

The Vehicular Ad-Hoc Network (VANET) is a dynamic network of vehicles and roadside units (RSUs) or infrastructures for ubiquitous wireless access. It primarily focuses on vehicle-to-vehicle (V2V) and vehicle-to-infrastructure (V2I) short-range communications that do not rely on base stations or wireless access points. Thus, VANET makes it convenient for inter-networking whenever any car joins or leaves the network regions. Based on VANET, various safety- and non-safety-related applications can be deployed to greatly enhance road travel and traffic/transportation efficiency [1]. This is possible by employing the IEEE 802.11p standard [2] that defines the physical (PHY) and medium access control (MAC) layers in the Dedicated Short Range Communications (DSRC) protocol stack for allowing vehicular communications in the 5.85–5.925 GHz range [3], [4]. In DSRC, the band is divided into seven channels of 10-MHz bandwidth each. One of the seven channels is used as the control channel (CCH) for safety messages transmission while the rest are used as service channels (SCH) for the non-safety information transmission.

Earlier research works have been devoted on studying broadcasting performance in VANETs [5], [6]. However, there are two main drawbacks when using this method.

First, due to the rapid change of network topology brought about by a large number of cars, broadcasting in VANET results in a mass of information packet collisions because of the simultaneous transmissions of messages. This is called broadcasting storm [7]. Second, broadcasting is incapable of ensuring the successful transmission without the transmission of acknowledgement (ACK) packets. Due to this limitation, broadcast is inadequate for transmitting some important data (could be safety or non-safety related) that requires automatic repeat request (ARQ) (e.g., 3D-point cloud sensor data for autonomous vehicles [8]). For these cases, unicast, instead of broadcast, is the preferred mode of transmission because there is a retransmission mechanism and confirmation procedure from the destination to the source node upon successful reception.

In the analysis of broadcasting performance in VANETs, the traffic mobility and distribution are assumed to be homogeneous and deterministic. However, it is evident that the dynamics of a vehicular network is mainly caused by the high mobility and uneven distribution of cars on the road. Therefore, incorporating practical and robust traffic models is critical in the analysis of vehicular networks. For example, such models can include a realistic vehicular traffic in signalized urban area and a heterogeneous assumption of vehicle distribution.

In this work, we tackle the research problem of unicast information exchange of data between vehicles through considering the influence of a realistic and practical vehicular flow. The traffic flow is captured by a stochastic traffic model that reflects the practical on-road vehicle distribution and the effect of traffic lights. Fig. 1 presents the proposed system block diagram for analyzing the 802.11p VANET unicast performance joint modeling and optimization.

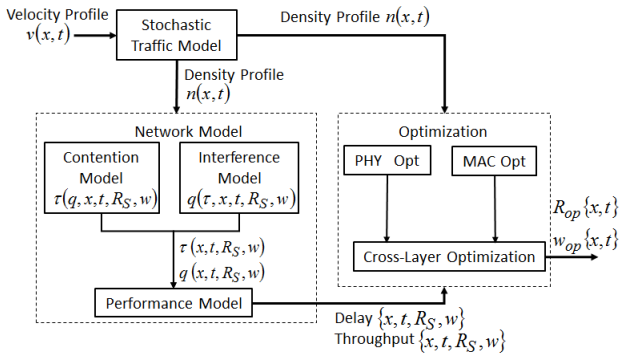

FIGURE 1. Block diagram for the methodology of 802.11p VANET unicast joint modeling and optimization.

Given the traffic velocity profile $v(x, t)$ as the system's input, the equivalent density profile $n(x, t)$ is derived by the Stochastic Traffic Model block. The Network Model block then computes the corresponding delay and throughput values at a certain location x, time t, transmission range R_S, and contention window size w. The 802.11p network channel access contention process of unicast is characterized in both the busy and idle channel states by using a two dimensional (2D) Markov chain-based contention model. On the other hand, we develop the interference model by analyzing packet collisions based on four possible scenarios involving the transmitting, receiving and interfering vehicles on the road. These delay and throughput values will be used to perform a cross-layer optimization to derive the optimal values of the transmission range R_{op} and contention window size w_{op} for location x and at time t. We validate the proposed system by performing extensive simulation and check whether it will provide realistic network performance results when using 802.11p unicast for V2V communications.

The remainder of this paper is structured as follows. Section II presents the related work for 802.11p VANETs vehicular traffic, network modeling, and optimization. Section III discusses our methodology by first presenting how a practical stochastic traffic model is developed. The section then presents the network model for 802.11p unicast by examining the contention and interference models. Cross-layer optimization is also tackled in this section. Section IV shows numerical results to validate our analytical models and the cross-layer optimization we introduced in obtaining optimal delay and throughput values. Discussion and future work can be seen in Section V. Finally, Section VI concludes our contribution.

II. BACKGROUND AND RELATED WORK

Most previous works in VANET performance analysis employed homogeneous road traffic scenario. The work in [6] generated highway traffic by following the freeway mobility model, where it assumes that the vehicle's current vehicle velocity is equal to its previous velocity. It also restricts that the following vehicle's velocity is less than that of the preceding vehicle. In [9] and [10], a one-dimensional (1D) highway traffic model is used for randomly distributing mobile vehicles following a Poisson distribution. The work in [11] studied high-density and low-density urban and highway traffic environments.

A more realistic approach is seen in [12] and [13]. Heterogeneity of vehicular flow is integrated in [12] by considering multiple entry/exit points on the highway. In [13], the heterogeneous traffic and density dynamics are characterized by a deterministic fluid dynamic model adhering to the conservation law. It also incorporated road intersections, and the density of cars in the jamming regions. However, the randomness of the individual vehicles and its effects among themselves, and the impact of traffic signaling lights are not evaluated. This is addressed in [14]. It modeled the vehicular traffic by utilizing a stochastic fluid dynamic to obtain a mean vehicular density profile. It also approximated the interaction between vehicles with the use of traffic lights on the road.

In modeling the 802.11p MAC-layer contention process to access the channel, the 2D Markov chain is utilized in most studies. Reference [15] analyzed the performance of 802.11 protocol by applying the 2D Markov chain to acquire a relationship between the transmission and collision

probabilities brought by concurrent transmitting and/or hidden nodes. Reference [16] also applied the 2D Markov chain to analyze the throughput of the Enhanced Distributed Channel Access (EDCA) mechanism in 802.11p VANET, then later improved the methodology in [15] by adding a retransmission limit. However, [15] and [16] did not consider the channel status (busy or idle) probability in the sensing process of a node. This limitation is incorporated in [17] and takes into account the augmentation of the multi-channel MAC protocol in IEEE 1609.4. The modeling of [15]–[17], however, did not bind vehicular networks with the practical traffic distribution in their contention modeling. On the other hand, [18] associated the 802.11p network under the saturation scenario with the practical stochastic traffic model in [14] to represent a contention model based on a 1D Markov chain. It evaluated the broadcasting efficiency of safety messages, i.e., ratio of the number of successful vehicular receptions and the total number of vehicles in the transmission region of a sender.

Network throughput and delay are the common metrics to measure VANET performance. Reference [15] calculated the mean delay as a set of expected time slots equal to the successful and failed packet transmission periods plus the idle period. Since 802.11 network is studied, it excluded the traffic distribution of nodes. [19] integrated the practical traffic model and network parameters when computing for the broadcasting delay and throughput. It also approximated the average contention time for accessing the channel.

When performing PHY-layer optimization, transmission power control technique is usually employed to tune the transmission range, minimize delay and avoid collisions. There are two methods for controlling the transmission power in a network, (1) local transmission power control, where each node can alter its own power level and (2) global transmission power control, where all nodes have identical transmitting power level. Local transmission power control is more effective than global transmission power control for PHY-layer optimization [20] because it is able to determine the number of neighboring nodes and packet reception rate (PRR). Obtaining the number of nodes in the vicinity is achieved via feedback-loop principle for slow-fading channel [21] or local neighbor discovery method [22]. However, the local neighbor discovery method fails to know the exact number of adjacent nodes due to interference. This deficiency is addressed in [7] by measuring the PRR. The PRR is defined as the ratio of the number of successfully received packets and the total number of packets sent. If the measured PRR is less (greater) than a threshold, then the transmission power of each vehicle is increased (decreased). Using these methods, on the other hand, produce additional delays and measurement overheads.

For MAC-layer optimization, classification of a service into different priority levels with different parameters is frequently utilized. Ma *et al.* [10] conceived a scheme to classify the safety service into three levels based on contention window sizes. This eliminates the inter-level countdown collisions for mending the broadcast reliability. In [23], the broadcasted safety service is sorted into several priority levels with different Arbitration Inter-Frame Space Number values. This ensures higher success rate for prioritized packets. However, the schemes in [10] and [23] are not suitable for unicast because of the presence of the ACK procedure and the classification of a service only increases the complexity of channel access contention. In addition, coordinating the sequence of nodes' transmissions optimizes the performance. In [24], the Self-organizing Time Division Multiple Access (STDMA) is proposed for coordinating safety data transmission slots for broadcasting between vehicles. Qiu *et al.* [19] estimated the throughput of a fully-coordinated broadcast scheme resembling the STDMA in [24] when distinct positions in the channel access queue are assigned to every vehicle. However, coordination-based methods are not appropriate for long multimedia stream unicast. If the transmission time is coordinated, one node waits for a long time before it can transmit, thus, instant messaging is not achieved.

There are various studies focusing on optimization methods that adjusts the parameters by measuring the network load. Shen *et al.* [25] improved the network throughput by developing an approach that measures the channel load congestion then adjusts the contention window size accordingly. Analogously, Hsu *et al.* [26] designed the Adaptive Offset Slot (AOS) mechanism to find the optimal contention window size by measuring the number of neighboring vehicles. In [27], performance-optimizing parameters are derived from a given a set of allowed contention window values. Rossi *et al.* [28] modeled the throughput between nodes by expressing it in terms of the control variable transmission probability and constant network parameters such as vehicle density, communication and interference ranges. Bianchi [15] and Patras *et al.* [29] employed adaptive techniques to tune the contention window size and achieve the optimal collision probability and transmission rate. Wang *et al.* [30] analytically represented the saturation throughput as a function of the contention window size. These methods derived the optimal value by obtaining the first derivative with respect to the control variable then equating to zero. All these discussed optimization approaches failed to include a realistic vehicular traffic flow in their models.

III. VEHICULAR TRAFFIC AND 802.11p NETWORK MODELING

In this section, we provide a detailed discussion on our proposed 802.11p VANET unicast joint modeling and optimization under the consideration of an urban traffic setup. We measure the network delay and throughput values from a given traffic velocity profile and later used these to obtain the optimal transmission range and contention window size for a certain location at a given time.

A. STOCHASTIC AND REALISTIC VEHICULAR TRAFFIC FLOW

An urban traffic is considered in this work, where the giant city-wide traffic road layouts between diverse constructions are composed of many roads crossing each other. The urban

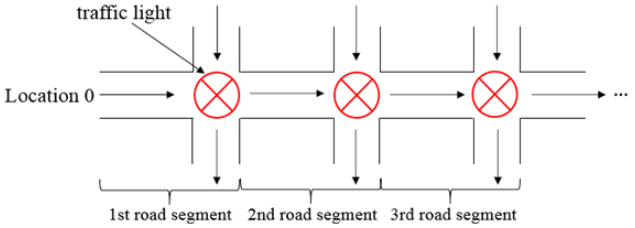

FIGURE 2. A single-lane and one-dimensional urban road scenario.

road can be split into numerous 1D roads that can be interpreted as a single-lane, one-directional, and semi-infinite scenario as depicted in Fig. 2.

A stochastic traffic model considering a 1D road system has two components, namely, (1) deterministic fluid dynamic model and (2) the stochastic model. With velocity profile, $v(x, t)$, as input (which can be obtained through inductive loop detector or traffic camera), the fluid model provides the knowledge regarding the average vehicular density, $n(x, t)$, through solving partial differential equation, while the distribution (or randomness) of the vehicular traffic is captured by the stochastic model. According to previous result, if the arrival of vehicles is Poisson distributed (which have been validated empirically in [14]), then the number of vehicles on a road segment is also Poisson distributed. Hence, via the stochastic traffic models, we can obtain the knowledge regarding the mean vehicular density and distribution as a function of space and time.

Given that the arrival process, $A(t)$, follows a nonhomogeneous Poisson distribution with an average arrival rate $\alpha(t)$, then, the number of vehicles, $N(x, t)$, in two non-overlapping regions $(x_1, x_2]$ and $(x_3, x_4]$ at time t are independent and can be expressed with means:

$$\bar{N}(x_1, x_2, t) = E[N(x_1, x_2)] = \int_{x_1}^{x_2} n(x, t)dx$$
$$\bar{N}(x_3, x_4, t) = E[N(x_3, x_4)] = \int_{x_3}^{x_4} n(x, t)dx \quad (1)$$

where $E[\bullet]$ is the expectation operator.

For further details regarding the stochastic traffic model, the reader is referred to [14].

B. THE NETWORK MODEL OF 802.11p VANET UNICAST

In this section, we derive the contention and interference models for implementing the 802.11p protocol in a vehicular network employing the unicast transmission. From these models and the derived vehicular density profile as its input, we evaluate the network performance by measuring its delay and throughput values.

1) THE CONTENTION MODEL OF 802.11p UNICAST

We model the contention process of channel access unicast transmissions in V2V communications of 802.11p VANETs. In this paper, we only focus on the packet transmission of the highest-priority access class, i.e., the single access class queue. We also only investigate the single-channel transmission for simplicity. Scenarios of multiple queues and/or multiple channels can be readily analyzed by extending our work. In the contention modeling approach, the network assumptions made are given in Table 1.

TABLE 1. 802.11p network model assumptions.

PHY Layer	1. The channel is isotropic and homogeneous along the one dimensional road. 2. Every vehicle has the same transmission range R_S and sensing/interference range R_I, where $R_S < R_I$. 3. Vehicles within the transmission range R_S of a transmitter are able to receive packets successfully if there is no collision. 4. Vehicles within the sensing/interference range R_I of a transmitting node can sense the transmission, and are interfered by the transmitter. 5. Transmission failure in the system is caused by packet collision only.
MAC Layer	1. The saturated condition, i.e., there are continuous packets available for transmissions during the service channels (SCH) interval, is considered to make a perpetual non-empty queue. 2. The channel time is regarded as infinitely long so that packet transmission will not be ceased due to channel switches [19]. 3. All nodes share the same EDCA setting.

Given that there is a car at location a (or simply car a), the 2D Markov chain to model the 802.11p unicast contention process of a single access class in the car according to the carrier-sense multiple access with collision avoidance (CSMA/CA) medium access mechanism is shown in Fig. 3. This model will be used to derive the probability τ for car a to transmit a packet at the beginning of a time slot.

To integrate the realistic traffic model with vehicular networks, the busy channel probability p is introduced because it is highly correlated to the vehicular traffic distribution. The contention model generates the transmission probability of a car as a function of the collision probability for the packet transmitted from the car. The arbitrary interframe space (AIFS) is omitted for convenience of analysis, but can be easily brought into the Markov chain by adding extra states. Note that every passing time slot in the Markov chain is the expected value of a busy time interval of T physical slots with probability p and an idle physical slot with probability $1 - p$. A physical slot here is equal to 16 μs [16]. The length of an expected time slot is equal to $pT + (1 - p)$ according to [19]. Table 2 gives the notations and definitions that are used in the 2D Markov chain.

The channel sensed by car a is busy if there is at least one car transmitting within its sensing range R_I. Thus, the busy channel probability p is found to be (2), assuming that the number of cars in the road is Poisson distributed and empirically verified in [14].

$$p = 1 - e^{-\bar{N}_{R_I}\tau_{R_I}} \quad (2)$$

where τ_{R_I} is the average transmission probability for all cars within car a's sensing range, and $\bar{N}_{R_I}$ is the mean number of cars in the sensing range of car a. Since an SCH interval of

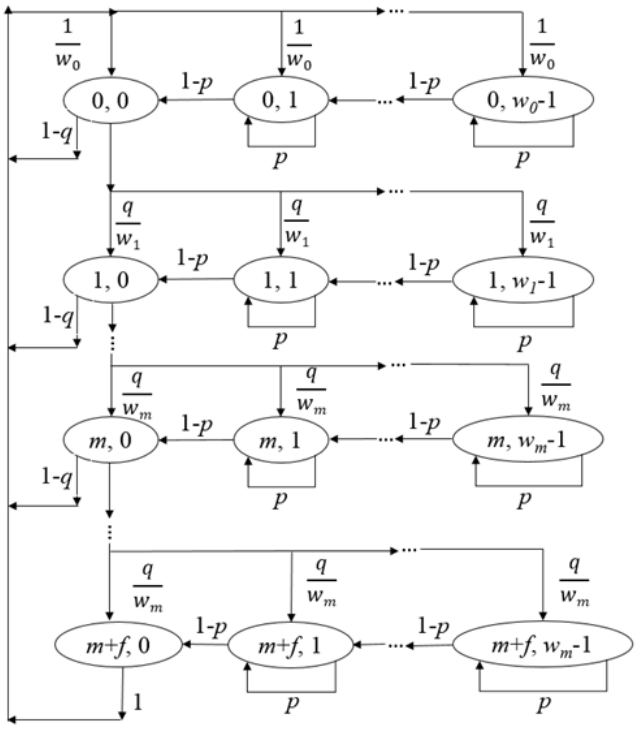

FIGURE 3. The 2D Markov chain for a single access class in 802.11p unicast.

TABLE 2. Notations used in the 2D Markov chain.

Notation	Definition
$< i, k >$	each state: i means the back-off stage (the number of collisions that one packet has suffered), and k is the back-off counter value
p	probability that the channel sensed by the car at a location is busy
w_i	the total number of counter values for the contention window size at stage i, and $w_i = CW_i + 1$
q	collision probability of the packet transmitted from the car at a location
m	maximum times for the initial contention window size to be doubled
f	maximum number of retransmissions after stage m and before the packet is discarded

50 ms is extremely small, the density profile $n(x, t)$ becomes $n(x)$ because the vehicular distribution can be seen as static during the SCH interval. From (1), we then have $\bar{N}_{R_I} = \int_{a-R_I}^{a} n(x)dx + \int_{a}^{a+R_I} n(x)dx$.

We solve the stationary distribution of the 2D Markov chain in Fig. 3 to obtain the transmission probability expression as a function of collision probability, given in (3).

$$\tau = \frac{1-q^{m+f+1}}{1-q}\left[\frac{1-q^{m+f+1}}{1-q} + \frac{1}{2(1-p)}\left(w_o\frac{1-(2q)^{m+1}}{1-2q} - \frac{1-q^{m+1}}{1-q}\right) + \frac{w_m-1}{2(1-p)}\left(\frac{q^{m+1}(1-q^f)}{1-q}\right)\right]^{-1} \tag{3}$$

If we set $m = 1$ and $f = \infty$ and permit packets to be retransmitted until successful reception by the receiver, we have (4) as the transmission probability τ of car a. The condition $m = 1$ and $f = \infty$ dictates that the contention window size is limited to be doubled only once upon a retransmission. It then stays constant at this doubled value even if there will be later retransmissions.

$$\tau = \frac{2(1-p)}{1-2p+w_0(1+q)} \tag{4}$$

where w_0 is a constant value from the EDCA settings.

2) THE INTERFERENCE MODEL FOR TRANSMISSIONS

In an earlier work [31], three interference regions are presented and analyzed. We extend the analysis to four regions by decomposing interference region 3 found in [31] to reveal the effects of hidden nodes.

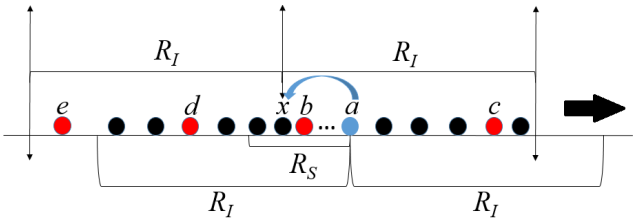

FIGURE 4. The Interference Scenario. Black arrow indicates the direction of vehicular flow.

We consider the scenario where a car in front is transmitting data to a car behind, e.g., car a to car x, as depicted in Fig. 4. In an ongoing unicast transmission from car a to car x, which is located within the transmission range R_S, if there is at least one car within the sensing range R_I of car x that is transmitting, then collision occurs at car x. Such transmitting car is called an interference source or interferer. In the scenario below, cars b, c, d and e are interferers, suggesting four non-overlapping regions to be analyzed. We model the interference by analyzing these four regions of interferers and their effect on the transmission of car a.

The interference probabilities for all four regions are synthesized and combined with the relationship in (4) to compute the collision probability q and the transmission probability τ.

As a general assumption, cars are arriving according to a Poisson process. The probability that there are i cars within car a's transmission range $[a - R_S, a)$ is given by (5).

$$P\{i \text{ cars in } [a-R_S, a)\} = \frac{(\bar{N}_{R_S})^i e^{-\bar{N}_{R_S}}}{i!} \tag{5}$$

where $0 \le i < +\infty$ and $\bar{N}_{R_S} = \int_{a-R_S}^{a} n(x)dx$ is the mean number of cars in the transmission range R_S of car a. A car k within the region $[a - R_S, a)$ has a probability $P(k) = 1/i$ to be randomly chosen as the receiver of car a, where $1 \le k \le i$.

a: INTERFERENCE REGION 1 (R1) $[a - R_S, a)$

In this region, the probability that there is at least one car, e.g., car b, transmitting can be expressed as (6).

$$B = 1 - \left(1 - \tau_{R_S}\right)^i \tag{6}$$

where τ_{R_S} is the average transmission probability of cars in Region 1. The probability that the k-th car receiver is interfered among i cars is (7).

$$P_{Intf\,1}(k) = P(k)B \tag{7}$$

The interference probability in R1, P_1, with i cars can be obtained by combining (5)–(7) and get (8).

$$\begin{aligned} P_1 &= \sum_{i=1}^{\infty} P\{i \text{ cars in R1}\} \sum_{k=1}^{i} P_{Intf\,1}(k) \\ &= 1 - e^{-\tau_{R_S}\bar{N}_{R_S}} \end{aligned} \tag{8}$$

b: INTERFERENCE REGION 2 (R2) $(a, x + R_I]$

Let $C(x)$ be the probability that at least one car, e.g., car c, transmits in R2 and be given by (9).

$$\begin{aligned} C(x) &= 1 - \sum_{n=0}^{\infty} P\{n \text{ cars in R2}\} P(n \text{ cars do not transmit}) \\ &= 1 - \sum_{n=0}^{\infty} \frac{(\bar{N}_C(x))^n e^{-\bar{N}_C(x)}}{n!} (1 - \tau_C)^n \\ &= 1 - e^{-\tau_C \bar{N}_C(x)} \end{aligned} \tag{9}$$

where $\bar{N}_C(x) = \int_a^{x+R_I} n(s)ds$ and τ_C are the average number of cars and average transmission probability of cars in R2, respectively. From [14], the probability density function (PDF) $f(x)$ for a car located at x within the transmission range $[a - R_S, a)$ can be identified given the vehicular density profile $n(x)$. $f(x)$ is given in (10).

$$f(x) = \begin{cases} \dfrac{n(x)}{\bar{N}_{R_S}} & a - R_S \le x < a \\ 0 & \text{otherwise} \end{cases} \tag{10}$$

The probability that the k-th car out of the i cars located at x, within the interval $[a - R_S, a)$, is interfered by transmitting cars in R2 is given in (11).

$$P_{Intf\,2}(k) = P(k) \int_{a-R_S}^{a} f(x)C(x)dx \tag{11}$$

The interference probability in R2, P_2, is obtained by combining (5) and (9)–(11), taking into consideration that receiver cars are chosen equiprobably. Thus, we get (12).

$$\begin{aligned} P_2 &= \sum_{i=1}^{\infty} P\{i \text{ cars in R1}\} \sum_{k=1}^{i} P_{Intf\,2}(k) \\ &= \frac{1 - e^{-\bar{N}_{R_S}}}{\bar{N}_{R_S}} \int_{a-R_S}^{a} n(x) \left[1 - e^{-\tau_C \bar{N}_C(x)}\right] dx \end{aligned} \tag{12}$$

c: INTERFERENCE REGION 3 (R3) $[a - R_I, a - R_S)$

Let D be the probability that at least one car, e.g., car d, transmits in R3. Similar to (9) in R2, we have:

$$\begin{aligned} D &= 1 - \sum_{n=0}^{\infty} P\{n \text{ cars in R3}\} P(n \text{ cars do not transmit}) \\ &= 1 - \sum_{n=0}^{\infty} \frac{(\bar{N}_D)^n e^{-\bar{N}_D}}{n!} (1 - \tau_D)^n \\ &= 1 - e^{-\tau_D \bar{N}_D} \end{aligned} \tag{13}$$

where $\bar{N}_D = \int_{a-R_I}^{a-R_S} n(s)ds$ and τ_D are the average number of cars and the average transmission probability of cars in R3, respectively.

The interference probability in R3, P_3, is obtained by combining (5) and (13) and still considering that receiver cars are chosen equiprobably. We then get (14).

$$\begin{aligned} P_3 &= \sum_{i=1}^{\infty} P\{i \text{ cars in R1}\} \sum_{k=1}^{i} P(k) D \int_{a-R_S}^{a} f(x)dx \\ &= \frac{(1 - e^{-\bar{N}_{R_S}})(1 - e^{-\tau_D \bar{N}_D})}{\bar{N}_{R_S}} \int_{a-R_S}^{a} n(x)dx \end{aligned} \tag{14}$$

d: INTERFERENCE REGION 4 (R4) $[x - R_I, a - R_I)$

Let $E(x)$ be the probability that at least one car, e.g., car e, transmits in R4. We have (15).

$$\begin{aligned} E(x) &= 1 - \sum_{n=0}^{\infty} P\{n \text{ cars in R4}\} P(n \text{ cars do not transmit}) \\ &= 1 - \sum_{n=0}^{\infty} \frac{(\bar{N}_E(x))^n e^{-\bar{N}_E(x)}}{n!} (1 - \tau_E)^n \\ &= 1 - e^{-\tau_E \bar{N}_E(x)} \end{aligned} \tag{15}$$

where $\bar{N}_E(x) = \int_{x-R_I}^{a-R_I} n(s)ds$ and τ_E are the average number of cars and average transmission probability of cars in R4, respectively.

From Fig. 4, all interferers are located beyond the sensing range of car a. They are considered as hidden nodes during the transmission of car a to car x and cause interference to car x. In R4, there are three cases involving the transmission of hidden nodes, namely: (1) hidden nodes and node a transmit simultaneously, (2) hidden nodes transmit before node a does, and (3) node a transmits before the hidden nodes do. Although hidden nodes and car a do not start transmitting concurrently in Cases 2 and 3, there still exist some overlapped transmission time slots as hidden nodes or car a begins to transmit in the midst of the transmission duration of each other.

For Cases 1 and 2, and from the time slot at which car a initiates the transmission, the probability that the k-th car-receiver located at x is interfered by transmitting nodes in R4 is determined by combining (10) and (15) and is given in (16).

$$P_{Intf\,4\_1}(k) = P(k) \int_{a-R_S}^{a} f(x)E(x)dx \tag{16}$$

For case 3, we consider the time slot when car a commenced its transmission and the state of each node (contending or transmitting) in the expected time slot $pT + (1 - p)$.

Let J be the number of expected slots needed to complete one practical transmission time of T physical slots. The hidden nodes will probably start transmitting at any one of the expected time slots of car a's transmission duration from the second slot to the J-th slot ($J \geq 2$). If the hidden nodes start transmitting at the second expected time slot of car a's transmission interval, it means that there is no car transmitting at the first expected time slot with the probability $1 - E(x)$. The probability that at least one hidden node transmits at the $(j + 1)$-th expected time slot in R4 is given by (17).

$$P_{exp}(j) = [1 - E(x)]^j E(x) \tag{17}$$

where $1 \leq j \leq J - 1$. Therefore, the conditional interference probability from R4 in Case 3 can be expressed as (18).

$$P_{Intf4\_2}(k) = P(k) \int_{a-R_S}^{a} f(x) \sum_{j=1}^{J-1} P_{exp}(j) dx \tag{18}$$

Therefore, the overall interference probability from R4 is given in (19).

$$\begin{aligned} P_4 &= \sum_{i=1}^{\infty} P\{i \text{ cars in R1}\} \sum_{k=1}^{i} \left[P_{Intf4\_1}(k) + P_{Intf4\_2}(k)\right] \\ &= C_4 \int_{a-R_S}^{a} \left[1 - e^{-\tau_E \bar{N}_E(x)}\right] \left[1 + \sum_{j=1}^{J-1} e^{-j\tau_E \bar{N}_E}(x)\right] dx \end{aligned} \tag{19}$$

where $C_4 = \frac{1-e^{-\bar{N}_{R_S}}}{\bar{N}_{R_S}} n(x)$ and $J = \lceil \frac{T}{pT+1-p} \rceil$. The $\lceil \bullet \rceil$ is the ceiling operator. Equation (19) shows the effect of the hidden nodes for the backward transmission. Note that if we also incorporate the forward transmission into the interference model, the interference probability from R4 will be higher as the hidden nodes' effect will be more significant.

Using P_1, P_2, P_3 and P_4, the collision probability, q, from car a to car x considering possible interferers in any of the four interference regions is (20).

$$q = 1 - (1 - P_1)(1 - P_2)(1 - P_3)(1 - P_4) \tag{20}$$

3) METRICS FOR NETWORK PERFORMANCE

The network performance of the 802.11p unicast is evaluated by measuring the expected delay and expected throughput.

The unicast delay is equivalent to the duration from the beginning of contention until the ACK signal is received after a successful packet reception. A successful transmission interval consists of a contention duration, a transmission duration, a Short Inter-Frame Space (SIFS) and an ACK transmission duration, while a failed transmission interval comprises only of the contention and transmission durations, as illustrated in Fig. 5. We assume that the maximum transmission range of the cars is 500 meters, thus, we can neglect the signal propagation time.

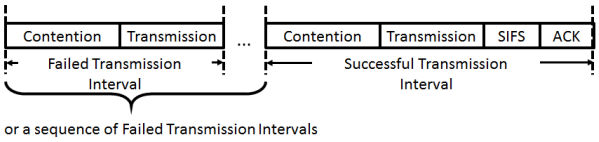

FIGURE 5. Unicast delay for a packet transmitted from a car.

A contention duration can be considered as a number of expected time slots, of which each is $pT + (1 - p)$ is based on the Markov chain. Here, T is a constant which denotes a transmission duration (the packets size/data rate). The contention duration, CD, is equal to α expected time slots before the car transmits, and has a probability:

$$P(CD) = (1 - \tau)^{\alpha} \tau \tag{21}$$

where τ is the transmission probability of the car.

The expected contention interval, $\overline{CT}$, is defined by:

$$\begin{aligned} \overline{CT} &= \sum_{\alpha=0}^{\infty} \alpha \left[pT + (1 - p)\right] (1 - \tau)^{\alpha} \tau \\ &= \left(\frac{1}{\tau} - 1\right) (pT - p + 1) \end{aligned}$$

Therefore, the total delay, D, shown in Fig. 5, can be expressed as (22).

$$D = \eta \underbrace{\left(\overline{CT} + T\right)}_{T_F} + \underbrace{\left(\overline{CT} + T + SIFS + ACK\right)}_{T_S} \tag{22}$$

where T_F and T_S are the intervals for failed and successful transmissions respectively, and η is the number of times a failed transmission occurred (due to collision).

The probability that there are η occurrences of collisions before a successful transmission is expressed as:

$$P\left(\eta \text{ collisions}\right) = q^{\eta}(1 - q)$$

Finally, the expected unicast delay, $E[D]$, is given by (23).

$$\begin{aligned} E[D] &= \sum_{\eta=0}^{\infty} D * P(\eta \text{ collisions}), \quad \eta \geq 0 \\ E[D] &= \frac{1}{1 - q} \left[\left(\frac{p}{\tau} - p + 1\right) T + \left(1 - \frac{1}{\tau}\right) p + \frac{1}{\tau} - 1\right] \end{aligned} \tag{23}$$

The SIFS and ACK transmission durations are left out since these are constant values.

From (23), the expected throughput of a car, $E[\rho]$, given a packet of size L, is shown in (24).

$$E[\rho] = \frac{L}{E[D]} \tag{24}$$

C. CROSS-LAYER OPTIMIZATION

The interference range strongly influences the network performance, as senders sense the channel within their own interference range before transmitting packets. Receivers also suffer from collisions on packet reception by concurrent

transmissions or the hidden-node corruption within the interference range. From [28] and [32], the relationship between a vehicle's transmission range R_S and interference range R_I is governed by (25).

$$R_I = \beta^{\frac{1}{\gamma}} R_S \tag{25}$$

where β is the signal-to-interference ratio (SIR) requirement and γ is the path-loss exponent with $\gamma > 2$. Therefore, adjusting the transmission range, R_S, by power control can accordingly tune the interference range, R_I, and improve the network performance.

The 802.11p MAC protocol has some limitations [25]. The internal collisions on packet transmissions within a node can be prevented by granting the transmission opportunity (TXOP) to the highest-priority service, however, the external collisions cannot be avoided. Additionally, there are deficiencies for using a fixed contention window size on all vehicles in unicast [30]. In a dense network, the probability of collisions increases because vehicles have an insufficient back-off period. On the other hand, in the case of a sparse network, vehicles will unnecessarily wait for too long for the back-off period causing an inefficient utilization of bandwidth. Therefore, the congestion control approach for MAC-layer optimization is to assign varying contention window sizes for vehicles at different locations according to the vehicular density in vicinity to drop external collision probability, thereby guaranteeing an efficient bandwidth utilization.

We propose and implement a novel cross-layer optimization on both the PHY- and MAC-layers for V2V communications without continuously monitoring and measuring its surrounding network load. This cross-layer optimization procedure determines the optimal transmission range first and then computes the contention window size on every location based on the given velocity profile.

1) PHY-LAYER OPTIMIZATION

PHY-layer optimization determines the optimal transmission ranges of vehicles for different locations, based on a given density profile. Network performance can be optimized by first reducing the transmission range, and then the interference range of each car while ensuring network connectivity. In this case, network connectivity requires that the distance, d, be less than or equal to R_S, and on the average must have one car on it to allow a single-hop interaction.

Based on the density profile $n(x)$ from the stochastic traffic model, we have the following expression below for vehicle a in a 1-connected network

$$\sum_{a-R_1}^{a} n(x)dx = 1 \tag{26}$$

where R_1 is the transmission range where there is only one car on average.

As $n(x)$ is the mean density, the expression in (26) has no means to ensure the network is connected. So, the optimal

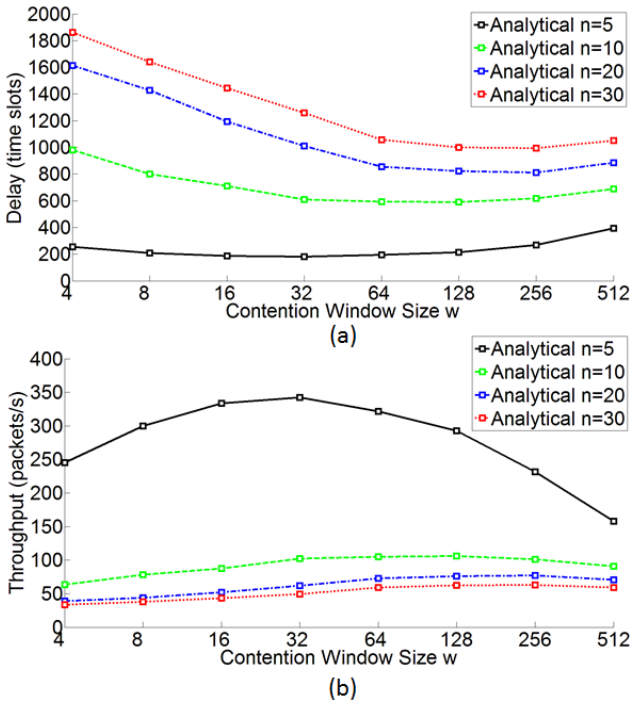

FIGURE 6. Analytical (a) delay performance and (b) throughput performance against the contention window size w for a homogeneous traffic.

transmission range R_{op} which can ensure the network connection can be decided as (27).

$$R_{op} = R_1 + \delta \tag{27}$$

The offset parameter $\delta = 0, 0.01, \ldots, 0.1$.

The road region [0, 4] km is divided into units of 0.01 km. For each δ, 3000 runs of simulations are performed to determine if the percentage of connected occurrences, P(con), (28), is greater than or equal to a threshold value of 0.8.

$$P(\text{con}) = \frac{\sum Occ_1}{\sum (Occ_1 + Occ_0)} \tag{28}$$

Occ_1 corresponds to a connected network while Occ_0 corresponds to a disconnected network.

If $P(\text{con}) \geq 0.8$, network connection is thought to be ensured. If the threshold is too high, the transmission range becomes very large; if the threshold is too low, the transmission range cannot ensure network connectivity.

For the value of δ that ensured connectivity, the optimal transmission range R_{op} at the location can be determined.

2) MAC-LAYER OPTIMIZATION

The optimal contention window size on every location controls the channel access contention in the MAC layer based on the network and stochastic traffic models.

Fig. 6 indicates the analytical distributions of delay and throughput at different contention window sizes for single access class queue in a homogeneous traffic. The network

parameters are $R_S = 0.2$ km, $R_I = 0.5$ km.The vehicular density, n, varies from 5 cars/km to 30 cars/km.

In a homogeneous traffic, we observe that when the contention window $4 \leq w \leq 512$, the network performance is unimodal, implying that the optimal contention window size, w_{op}, is within the interval [4, 512]. If the density is high, w_{op} becomes larger as longer contention time is demanded to minimize collisions. On the other hand, if the density is low, w_{op} becomes smaller to reduce unwanted waiting time before the transmission. Algorithm 1 details the steps undertaken to find the optimal contention window size, w_{op}, from the interval [4, 512].

Note that, at different locations, the interference ranges of the potential receivers may be different since the optimal transmission ranges are possibly different. Therefore, the interference regions should be adjusted accordingly if the interference range of the receiver is different from that of the sender.

Moreover, hidden nodes beyond the sensing/interference range of the transmitter can probably sense the transmitter because those hidden nodes can have larger sensing ranges than the transmitter's after the transmission range adjustment. In such cases, Case 3 will not take place and will be ignored in computing the collision probability of the packet transmission from the transmitter.

IV. SIMULATION SETUP AND NUMERICAL RESULTS

Exhaustive simulations are performed using C++ to validate the analytical modeling and optimization of 802.11p VANETs unicast performance. The simulation framework includes two parts, namely traffic and network simulations.

A. VEHICULAR TRAFFIC AND NETWORK SIMULATION SETUP

Homogeneous and nonhomogeneous traffic scenarios are considered. For a homogeneous situation, vehicular density, $n(x)$, is varied from 5 cars/km to 30 cars/km. In the heterogeneous condition, vehicles arrive at Location $x = 0$ (in Fig. 2) according to a Poisson process having an arrival rate of 12 cars/min. The traffic signal is situated at $x = 2$ km and is red during the time interval (4, 4.5] min. When the traffic light turns red, the vehicles' mean free speed, $v_f(x, t)$, is given by (29), where $v = 1$ km/min [14].

$$v_f(x,t) = \begin{cases} v & x < 1.98 \\ \left(\frac{v}{0.02}\right)(2-x) & 1.98 \leq x < 2 \\ 0 & 2 \leq x < 2.012 \\ \left(\frac{v}{0.02}\right)(x-2.012) & 2.012 \leq x < 2.032 \\ v & x \geq 2.032 \end{cases} \quad (29)$$

Car interactions are incorporated into the simulation by using the revised Greenshield's model (30)

$$v(x,t) = v_f\left(1 - \frac{n(x+\Delta x, t)}{k_j}\right) \quad (30)$$

Algorithm 1 Finding w_{op} Within the Range [4, 512]

for $w = 4; w \leq 512; w = 2w$ **do**
  $D[0.5w]$ = Analytical model$(n(x), R_S, 0.5w)$
  $D[w]$ = Analytical model$(n(x), R_S, w)$
  $D[2w]$ = Analytical model$(n(x), R_S, 2w)$
  if $(D[0.5w] > D[w])$ AND $(D[w] < D[2w])$ **then**
    $D_m = D[w]$
    $D_1 = D[0.5w]$
    $D_2 = D[2w]$
    $w_m = w$
    $w_1 = 0.5w$
    $w_2 = 2w$
  end if
end for
Implement quadratic curve fitting on (w_1, D_1), (w_m, D_m) and (w_2, D_2) to obtain a provisional delay function: $D(w) = a_1 w^2 + a_2 w + a_3$.
w_{op} = round$(-\frac{a_2}{2a_1})$.
if $(w_{op}==w_m)$ **then**
  $D[w_m - 1]$ = Analytical model$(n(x), R_S, w_m - 1)$
  $D[w_m + 1]$ = Analytical model$(n(x), R_S, w_m + 1)$
  if $(D[w_m - 1] > D_m)$ AND $(D_m < D[w_m + 1])$ **then**
    $D_{op} = D_m$
    Output: w_{op}, D_{op}. ▷ Optimal values are found.
    BREAK; ▷ Algorithm ends.
  else if $(D[w_m - 1] > D_m)$ AND $(D_m > D[w_m + 1])$ **then**
    $w_1 = w_m, w_m = w_m + 1$
    $D_1 = w_m, D_m = D[w_m + 1]$
  else
    $w_2 = w_m, w_m = w_m - 1$
    $D_2 = w_m, D_m = D[w_m - 1]$
  end if
  if $(w_1 == w_m - 1)$ AND $(w_2 == w_m + 1)$ **then**
    $w_{op} = w_m, D_{op} = D_m$
    Output: w_{op}, D_{op}. ▷ Optimal values are found.
    BREAK; ▷ Algorithm ends.
  end if
  Iterate from Step 14.
end if
D_{op} = Analytical model$(n(x), R_S, w_{op})$
if $(D_{op} < D_m)$ **then**
  if $(w_{op} < w_m)$ **then**
    $w_2 = w_m, w_m = w_{op}, D_2 = D_m, D_m = D_{op}$
  else
    $w_1 = w_m, w_m = w_{op}, D_1 = D_m, D_m = D_{op}$
  end if
  if $(w_1 == w_m - 1)$ AND $(w_2 == w_m + 1)$ **then**
    $w_{op} = w_m, D_{op} = D_m$
    Output: w_{op}, D_{op}. ▷ Optimal values are found.
    BREAK; ▷ Algorithm ends.
  end if
  Iterate from Step 14.
else
  if $(w_{op} < w_m)$ **then**
    $w_1 = w_{op}, D_1 = D_{op}$
  else
    $w_2 = w_{op}, D_2 = D_{op}$
  end if
  if $(w_1 == w_m - 1)$ AND $(w_2 == w_m + 1)$ **then**
    $w_{op} = w_m, D_{op} = D_m$
    Output: w_{op}, D_{op}. ▷ Optimal values are found.
    BREAK; ▷ Algorithm ends.
  end if
  Iterate from Step 14.
end if

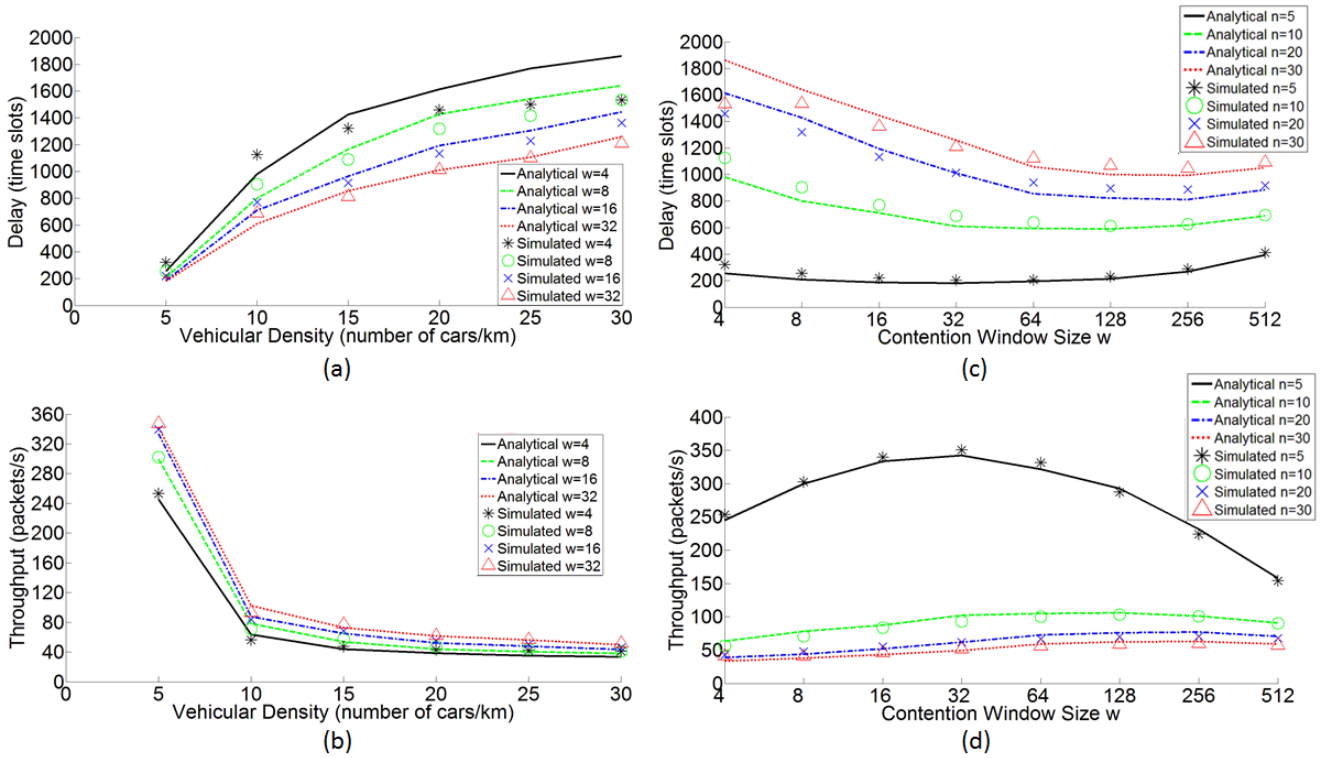

FIGURE 7. Analytical and simulated delay and throughput performance against the vehicular density (a)-(b) and contention window size (c)-(d) for homogeneous traffic.

where k_j is the jamming density equal to 500 cars/km and $\Delta x = 0.02$ km.

We run the heterogeneous traffic scenario simulation for 3000 rounds with different random seeds to obtain the mean vehicular density profile for approximation of the stochastic traffic model.

The single-queue transmission on a single channel network is simulated after the traffic simulation results are obtained. For the homogeneous case and at each density level, 100 simulation rounds are run to estimate the network performance. For the heterogeneous case and for every round of the 3000 traffic simulation trials, the vehicular distribution on each road unit spaced at 0.01 km are varied.

We run the network simulations for 500 channel intervals for each traffic simulation round to acquire the average delay, D_{ave}, (average throughput, $Tput_{ave}$) for one packet transmitted from cars on a road unit as follows,

$$D_{ave} = \frac{\sum_{N=1}^{500} time(N)}{\sum_{N=1}^{500} SucNo(N)} = \frac{1}{Tput_{ave}} \tag{31}$$

where N denotes each channel interval, $time(N)$ is the total time for packets transmissions and $SucNo(N)$ is the number of packets successfully transmitted in the N-th channel interval. This is done at every location on the traffic route.

Table 3 lists all the parameters used for the analysis and simulation in this paper. We set the path-loss exponent $\gamma = 2.5$ and the SIR requirement $\beta = 10$ dB to have $R_I = 2.5R_S$

TABLE 3. Network simulation parameters.

Parameter	Value
Transmission Range, R_S	0.2-0.5 km, optimal values in different scenarios
Interference Range, R_I	$2.5R_S$
Total number of counter values, w	4,8, 16, 32, optimal values in different scenarios
Time slot	16 μs
Packet size	512 bytes
Data rate	6 Mbps
SCH time	50 ms

according to (25). The packet, of which the transmission has not yet finished when the SCH interval expires, will be abandoned as there will be newly generated packets in the next SCH interval. This implies that the maximum value of delay for a packet should not be larger than a channel time interval of SCH, i.e., 3125 time slots (50 ms/16μs).

B. PERFORMANCE EVALUATION OF 802.11p VANETs UNICAST

Fig. 7 (a)-(b) show the analytical and simulated results of delay and throughput for the homogeneous traffic distribution, when transmission range $R_S = 0.2$ km. For the single queue at each contention window size, the delay is monotonically increasing, (monotonically decreasing for the throughput), when the number of vehicles becomes more dense. This is due to the fact that the average contention time of

a node for channel access becomes longer and the collision probability for packet transmissions gets higher.

When the contention window size is increased, delay decreases (throughput increases) because the exponential back-off procedure in unicast ensures the that there is an adequate waiting time for nodes before transmitting, thereby, avoiding potential collisions during transmissions.

Additionally, when the contention window size increases to an excessively large value, delay will become longer (throughput will drop), as shown in Fig. 7 (c)-(d).

For heterogeneous traffic, the vehicular density profile changes as time goes. After 3000 heterogeneous traffic simulation rounds, the mean vehicular density profile $n(x)$ captured at time $t = 4.5$ min in the road region [0, 4 km] is shown in Fig. 8.

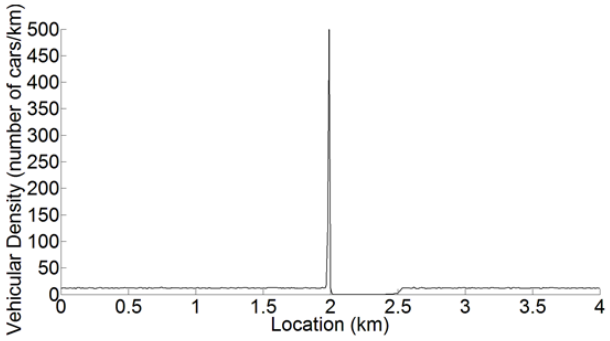

FIGURE 8. The mean vehicular density profile at different locations captured at time $t = 4.5$ min.

From the simulated vehicular density profile above, the delay and throughput results given a nonhomogeneous traffic situation are illustrated in Fig. 9.

In the region before 1.46 km, the packet transmission delay is roughly constant regardless of the contention window sizes, because the traffic distribution is equal to 12 cars/km and still far from the interference region.

From this region, the delay starts to increase since cars are now within the sensing/interference ($R_I = 0.5$ km) range from the point where traffic is starting to build up, i.e., $x_{buildup} = 1.96$ km. In such scenario, there will be longer contention time and more collisions because of the formation of a platoon of vehicles within the interference range. At some point, the delay sharply declines beyond the peak location as there is a substantial decrement on the vehicular density because of the zero-density zone after the traffic signal. In the road region of (2.53 3.03] km, the delay gradually increases because vehicles are piling upon exiting the zero-density zone, and are still within the interference range of the transmitting cars. Finally, a constant delay is again demonstrated because of a homogeneous vehicular distribution with density of roughly 12 cars/km within the region from location 2.53 km, in which all the possible hidden nodes are located for the transmitters.

Just like the homogeneous case, to reduce (increase) delay (throughput), the contention window size must be increased.

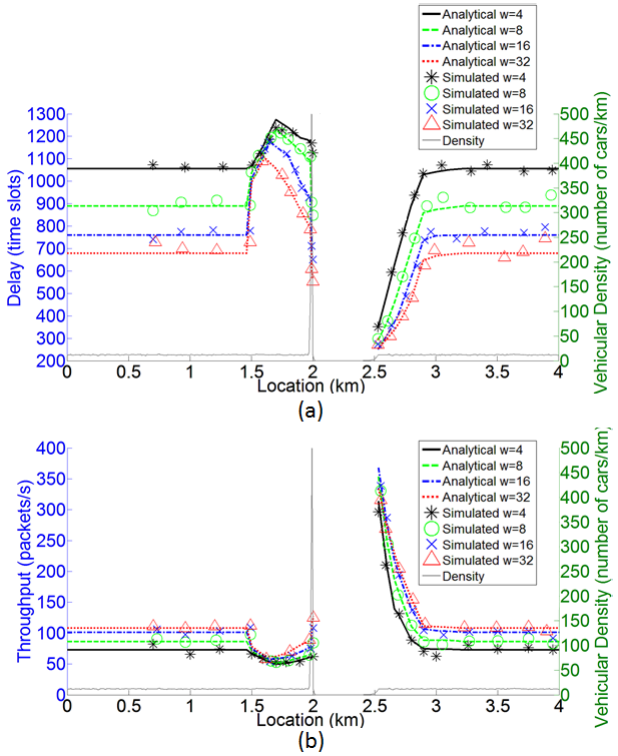

FIGURE 9. Analytical and simulated delay (a) and throughput (b) performance against the location for heterogeneous traffic.

TABLE 4. K-S test results for analytical and simulated delay and throughput in homogeneous traffic.

	w=4	w=8	w=16	w=32	Row-wise average value
K-S result	0.5	0.33	0.17	0.17	0.29
h	0	0	0	0	0
p-value	0.32	0.81	0.99	0.99	0.78

Therefore, we can say that the heterogeneous vehicular distribution on a road with the signal control also has a strong influence on unicast performance, e.g., rise in delay due to the rise of vehicular density.

Moreover, the availability of the network model based on the stochastic traffic model for homogeneous and heterogeneous traffic is verified by the presence of the small deviation between the analytical and simulated results. However, the difference is a bit larger at the high contention window size, say 32, which purports that our model is more accurate for evaluating the network performance of unicast transmissions with low contention window sizes.

The Kolmogorov-Smirnov test (K-S test) [33] is conducted to inspect the goodness of fit between the analytical results and the simulated results for quantifying the accuracy of our analytical model. The results of the K-S tests for homogeneous and heterogeneous traffic are given in Tables 4-6.

C. CROSS-LAYER OPTIMIZATION RESULTS

The contention window size is fixed at $w = 4$ at various vehicular densities. Fig. 10 shows the simulated delay

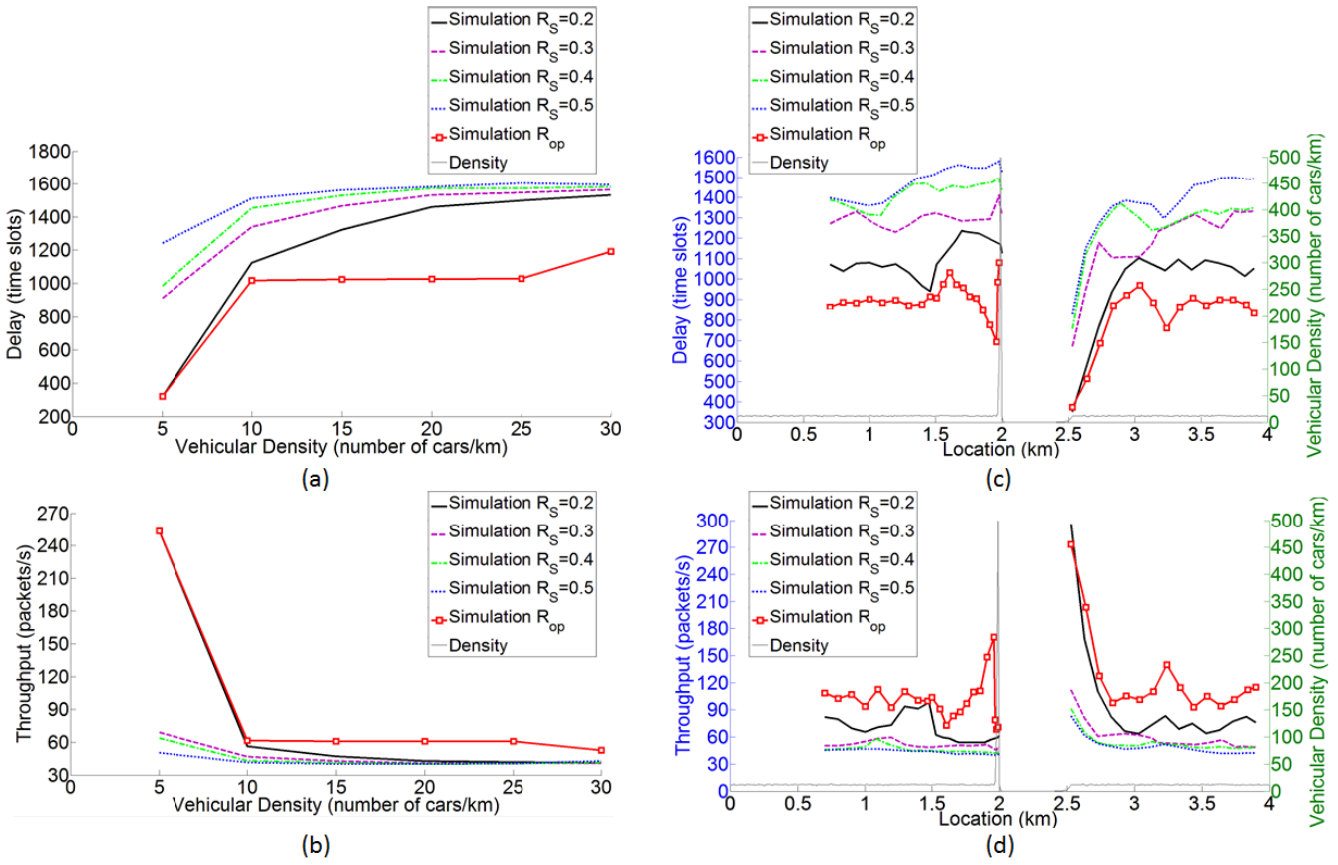

FIGURE 10. Simulated delay and throughput performance results of the PHY-layer optimization for homogeneous (a-b) and heterogeneous (c-d) traffic.

TABLE 5. K-S test results for analytical and simulated delay and throughput in heterogeneous traffic.

	w=4	w=8	w=16	w=32	Row-wise average value
K-S result	0.24	0.22	0.27	0.33	0.27
h	0	0	0	0	0
p-value	0.53	0.59	0.33	0.15	0.4

TABLE 6. K-S test results for analytical and simulated throughput in heterogeneous traffic.

	w=4	w=8	w=16	w=32	Row-wise average value
K-S result	0.21	0.21	0.28	0.35	0.26
h	0	0	0	0	0
p-value	0.74	0.74	0.43	0.19	0.53

and throughput performance results when the PHY-layer is optimized for the single access data queue for both the homogeneous and heterogeneous traffic. With the optimal transmission ranges, R_{op}, the delay is lowest and the throughput outperforms the fixed transmission ranges performance. From Fig. 10 (a)-(b), the optimal delay and throughput are unchanged for a wide range of car densities, (10 cars/km $\leq$ $n(x) \leq$ 25 cars/km). This is achieved by adaptively changing the transmission range to make sure that on the average the degree of connectivity is one.

For a heterogeneous traffic, depicted in Fig. 10 (c)-(d), almost the same observations can be made, however, we note that there is a sudden increase in optimal delay (decrease in throughput) near the traffic light, which is extraordinarily dissimilar compared with the original network performance trend. This is due to the exceedingly high congestion density in front of the traffic light, by which the optimal transmission ranges close to the traffic signal are too small, and the corresponding sensing ranges are also very limited. These result in much more collisions caused by an increasing number of hidden nodes out of the small sensing ranges of the transmitters.

Furthermore, it is also noteworthy to say that the optimal delay (throughput) is higher (lower) than the original delay (throughput) values with transmission range 0.2 km around location 2.5 km. For this case, the density is very low by which the optimal transmission/sensing ranges are relatively large for ensuring the network connection. Cars at that location sense more transmitting nodes and experience longer busy time on the channel before packet transmission. These findings, in general, verify that the PHY-layer optimization is workable.

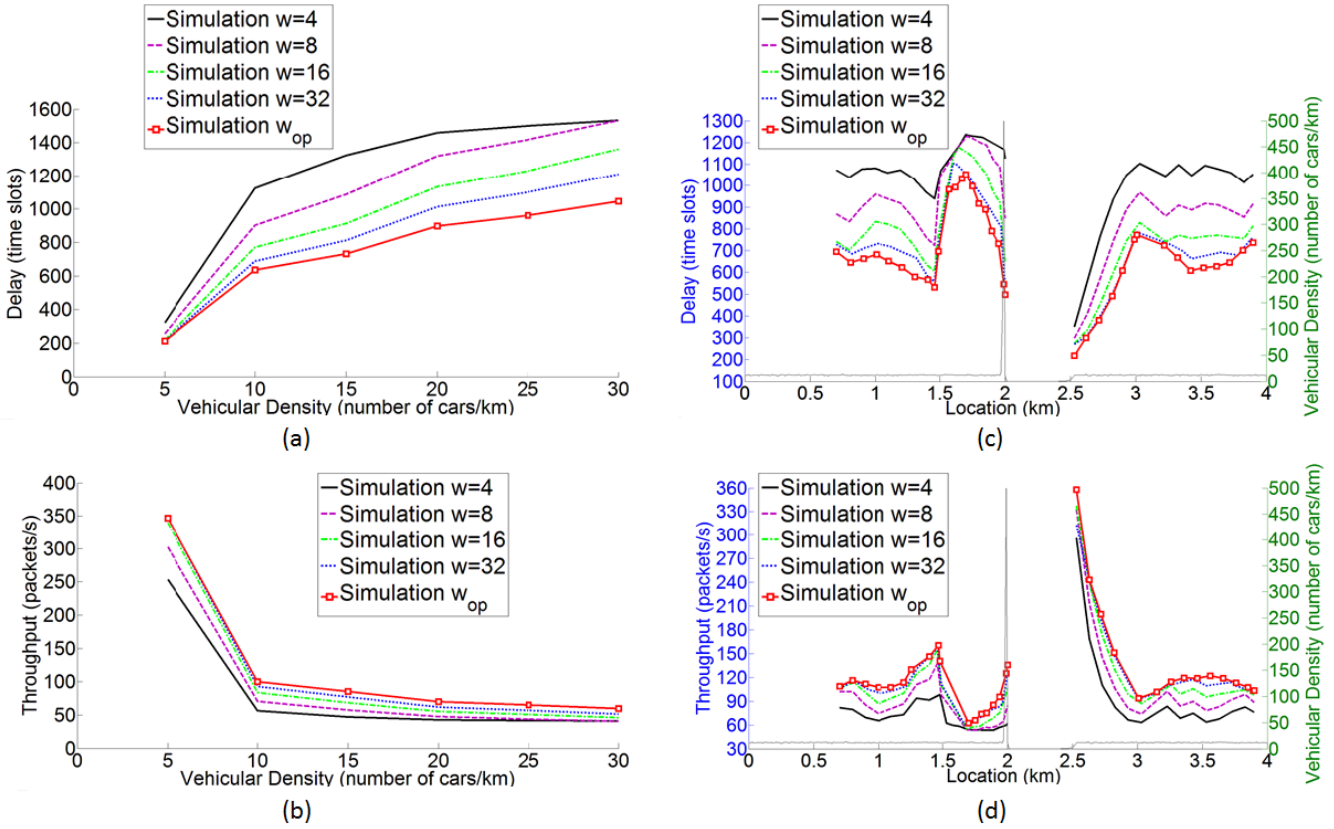

FIGURE 11. Simulated delay and throughput performance results of the MAC-layer optimization for homogeneous (a-b) and heterogeneous (c-d) traffic.

Fig. 11 displays the simulated delay and throughput performances for homogeneous and nonhomogeneous traffic when MAC-layer optimization on the single data queue transmission is employed. For varying car distributions, the contention window size w_{op} varies optimally at every location to achieve low delay and high throughput. In MAC-layer optimization, the transmission range is fixed to 0.2 km.

We now perform the cross-layer optimization for the single access class queue. The network performance results are shown in Fig. 12 and compared to the benchmark that uses a transmission range $R_S = 0.2$ km and a contention window size $w = 4$. The previous PHY-layer optimization performance results and MAC-layer optimization performance indexes in both homogeneous and heterogeneous traffic are also included.

In general, the MAC-layer optimization provides a higher performance improvement than the PHY-layer optimization. With this, we add the robustness that the PHY-layer optimization brings so that a wide range of vehicular densities will have the same delay and throughput performance. By executing a cross-layer optimization in a homogeneous traffic scenario, the unicast delay is reduced on the average by 53% while the throughput is increased by about 120% when compared to the benchmark (with $R_S = 0.2$ km and $w = 4$). On the other hand, for a heterogeneous traffic, the delay decreases by approximately 45% while the throughput is roughly 104% higher on average.

In summary and with reference to Fig. 1, as vehicles enter Location 0 in Fig. 2, the empirical spatio-temporal velocity profile is monitored, e.g., through inductive loop detector or traffic camera. We exploit the stochastic traffic model and respective 802.11p unicast model to obtain the network performance profile as a function of space and time for network optimization. The computed optimal values (also functions of space and time) are disseminated to the vehicles through roadside units (RSUs) when they enter a particular road segment. Hence, continuous monitoring of neighboring vehicles need not be done by individual vehicles.

V. DISCUSSION

Simulations have verified the analytical models and optimization methods in unicast performance. The stochastic model that has been incorporated in this study follows a Poisson distribution with an empirical validation coming from Central London [14]. We wish to extend the findings in this work to other traffic distributions that do not follow our setup. For example, Zhang *et al.* [34] demonstrated that the lane-level traffic in Shanghai followed the Gaussian distribution and is dependent on each road segment. Also, we aim to extend our stochastic traffic model to the two-dimensional traffic road with complex road topologies including multiple directions and lanes, curvatures and gradients, etc. Another traffic research issue that can be explored is the burst traffic [35] that can cause sudden topology changes. Moreover, multi-channel

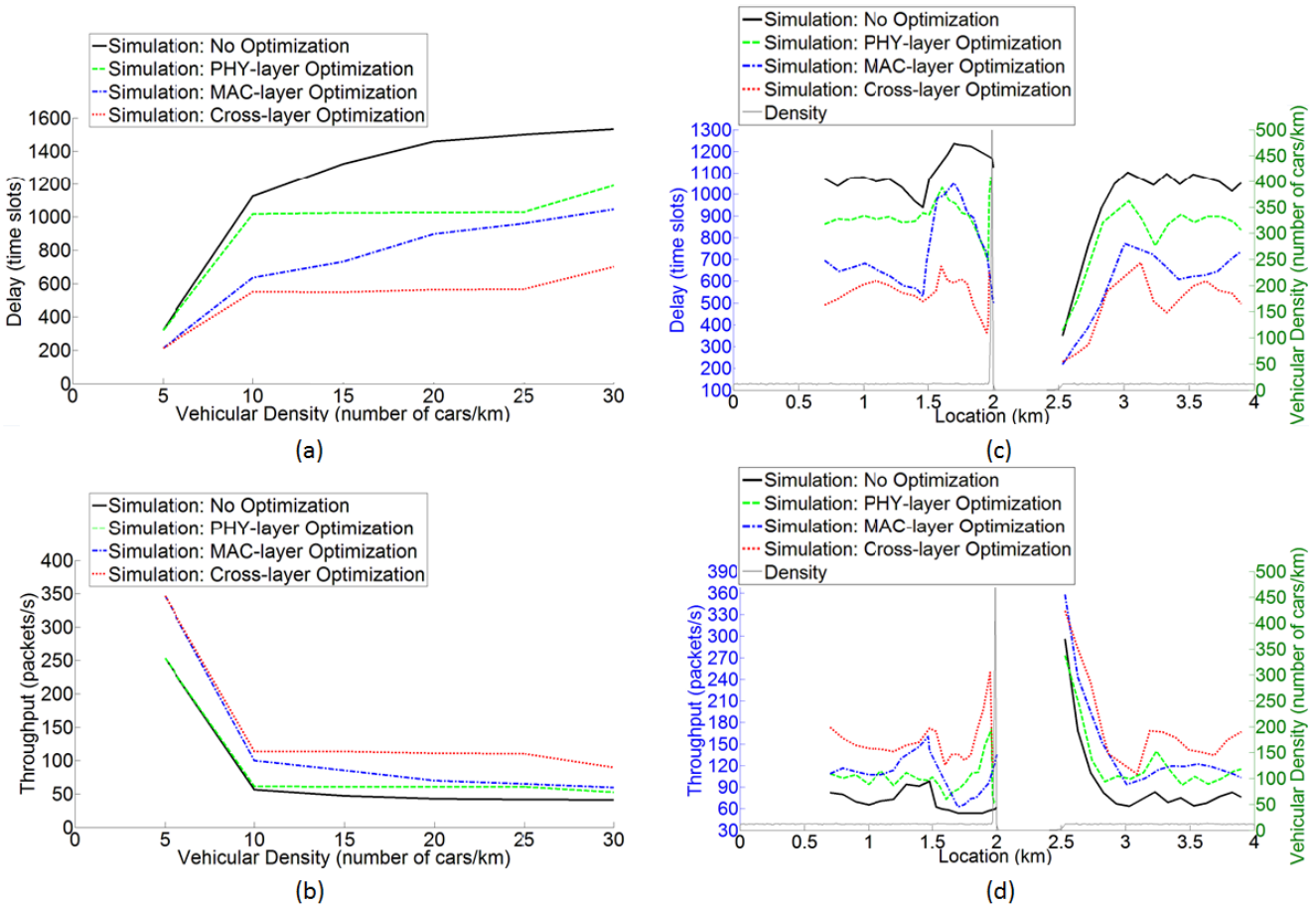

FIGURE 12. Simulated delay and throughput performance results of the cross-layer optimization for homogeneous (a-b) and heterogeneous (c-d) traffic.

transmissions with multiple access classes should be modeled to overcome the shortage that there is only single access classes queue transmitted on single channel being considered.

We have also shown how collision affects the unicast performance in our simulations. From these, other factors such as channel coding error, loss of packets, bit error and fading can now be included and studied. Throughput performance can be further enhanced (or diminished) by using packets of variable lengths, where the packet size is application-dependent. An adaptive data rate can also be set to increase throughput.

In addition, the performance curves under MAC-layer optimization illustrated a unimodal behavior. We can explore other standard searching methods such as golden section search [36] to identify the optimal contention window size more efficiently. Adjustments in AIFS, [27] and control channel (CCH)/SCH interval [4] are also included in further research activities.

The future works related to 802.11p VANETs modeling and optimization primarily includes three aspects beneath:

1) The V2I communication and optimization with rational deployment of infrastructures ought to be analyzed. This will build a comprehensive analytical model of VANET's performance together with the V2V model done in this paper. We can refer to the novel V2I hybrid optimization method named Dynamic Resources Allocation Scheme (DRAS) proposed in [37].
2) We can investigate the performance of existing routing protocols in VANETs, e.g., DSDV, OLSR, AODV, and DSR [38], and decide the proper one to be used for different vehicular density levels. As routing protocols are fundamental for Quality of Service (QoS) enhancement, the optimization for routing protocols should be brought to the forefront.
3) We can apply cooperative communications on VANETs for promoting reliability of transmission links. As an illustration, [39] proposed the cooperative ad-hoc MAC (CAH-MAC) protocol in which vicinal nodes cooperate in retransmitting failed packets in previous transmissions due to poor channel condition. The cooperation implemented in unreserved time slots could mitigate the dissipation of time slots, enhance network throughput, and debase the packet dropping rate.

VI. CONCLUSION

In this paper, a stochastic vehicular traffic model has been used to evaluate the performance of unicast in 802.11p

VANETs for V2V communications. It allowed our methodology to capture the random characteristics of real-world vehicle motions in a signalized urban traffic area. Based on the stochastic traffic model, a 2D Markov chain is employed to depict the channel access contention for transmissions of a node at a certain location in the network. Respective interference model that characterizes the effect of packet collisions has also been developed.

By jointly solving the node's transmission and collision probabilities, the network performance, in terms of expected unicast transmission delay and throughput can be obtained. The proposed analytical models have been validated through extensive simulation, and our results confirmed that the proposed models can accurately predict vehicular network performance. Hence, related network planning and optimization can be carried out to achieve higher network efficiency.

Based on the network performance profile obtained from the analytical models, we have proposed cross-layer optimization methods to further improve the network performance. As an advantage, the vehicles can obtain the optimal network configurations from RSUs and directly set in advance their transmission ranges and contention window sizes to the optimal values before moving into a particular road region.

Overall, given the velocity profile of vehicles as the input, the delay, throughput and the optimized performance with the optimal transmission ranges and contention window sizes can be readily computed as a function of space and time according to a set of models and methodologies proposed in this paper. Our analytical models and the corresponding optimization methods can provide insights into the future design and evaluation of other communication protocols in VANETs.

REFERENCES

[1] N. S. Nafi and J. Y. Khan, "A vanet based intelligent road traffic signalling system," in *Proc. Austral. Telecommun. Netw. Appl. Conf. (ATNAC)*, 2012, pp. 1–6.

[2] *Wireless LAN Medium Access Control (MAC) and Physical Layer (PHY) Specifications*, IEEE Standard 802.11-1997, 1997.

[3] D. Jiang and L. Delgrossi, "IEEE 802.11p: Towards an international standard for wireless access in vehicular environments," in *Proc. IEEE Veh. Technol. Conf. (VTC Spring)*, May 2008, pp. 2036–2040.

[4] J. Misic, G. Badawy, S. Rashwand, and V. B. Misic, "Tradeoff issues for CCH/SCH duty cycle for IEEE 802.11p single channel devices," in *Proc. IEEE Global Telecommun. Conf. (GLOBECOM)*, Dec. 2010, pp. 1–6.

[5] H. A. Omar, W. Zhuang, and L. Li, "VeMAC: A TDMA-based MAC protocol for reliable broadcast in VANETs," *IEEE Trans. Mobile Comput.*, vol. 12, no. 9, pp. 1724–1736, Sep. 2013.

[6] C. Wu, X. Chen, Y. Ji, S. Ohzahata, and T. Kato, "Efficient broadcasting in VANETs using dynamic backbone and network coding," *IEEE Trans. Wireless Commun.*, vol. 14, no. 11, pp. 6057–6071, Nov. 2015.

[7] O. Chakroun, S. Cherkaoui, and J. Rezgui, "MUDDS: Multi-metric unicast data dissemination scheme for 802.11p VANETs," in *Proc. 8th Int. Wireless Commun. Mobile Comput. Conf. (IWCMC)*, Aug. 2012, pp. 1074–1079.

[8] K. F. Chu, E. R. Magsino, I. W.-H. Ho, and C.-K. Chau, "Index coding of point cloud-based road map data for autonomous driving," in *Proc. IEEE Veh. Technol. Conf. (VTC)*, Jun. 2017.

[9] X. Ma and X. Chen, "Delay and broadcast reception rates of highway safety applications in vehicular ad hoc networks," in *Proc. Mobile Netw. Veh. Environ.*, May 2007, pp. 85–90.

[10] X. Ma, J. Zhang, X. Yin, and K. S. Trivedi, "Design and analysis of a robust broadcast scheme for VANET safety-related services," *IEEE Trans. Veh. Technol.*, vol. 61, no. 1, pp. 46–61, Jan. 2012.

[11] M. J. Booysen, S. Zeadally, and G.-J. Van Rooyen, "Performance comparison of media access control protocols for vehicular ad hoc networks," *IET Netw.*, vol. 1, no. 1, pp. 10–19, 2012.

[12] M. Khabazian and M. K. M. Ali, "A performance modeling of connectivity in vehicular ad hoc networks," *IEEE Trans. Veh. Technol.*, vol. 57, no. 4, pp. 2440–2450, Jul. 2008.

[13] T. Umer, Z. Ding, B. Honary, and H. Ahmad, "Implementation of microscopic parameters for density estimation of heterogeneous traffic flow for VANET," in *Proc. 7th Int. Symp. Commun. Syst. Netw. Digital Signal Process. (CSNDSP)*, 2010, pp. 66–70.

[14] I. W.-H. Ho, K. K. Leung, and J. W. Polak, "Stochastic model and connectivity dynamics for VANETs in signalized road systems," *IEEE/ACM Trans. Netw.*, vol. 19, no. 1, pp. 195–208, Feb. 2011.

[15] G. Bianchi, "Performance analysis of the IEEE 802.11 distributed coordination function," *IEEE J. Sel. Areas Commun.*, vol. 18, no. 3, pp. 535–547, Mar. 2000.

[16] C. Han, M. Dianati, R. Tafazolli, R. Kernchen, and X. Shen, "Analytical study of the IEEE 802.11p MAC sublayer in vehicular networks," *IEEE Trans. Intell. Transp. Syst.*, vol. 13, no. 2, pp. 873–886, Jun. 2012.

[17] Q. Wang, S. Leng, H. Fu, Y. Zhang, and H. Weerasinghe, "An enhanced multi-channel MAC for the IEEE 1609.4 based vehicular ad hoc networks," in *Proc. IEEE Conf. Comput. Commun. Workshops (INFOCOM)*, Mar. 2010, pp. 1–2.

[18] H. J. F. Qiu, I. W.-H. Ho, and K. T. Chi, "A stochastic traffic modeling approach for 802.11p VANET broadcasting performance evaluation," in *Proc. IEEE 23rd Int. Symp. Pers. Indoor Mobile Radio Commun. (PIMRC)*, Sep. 2012, pp. 1077–1083.

[19] H. J. F. Qiu, I. W.-H. Ho, K. T. Chi, and Y. Xie, "A methodology for studying 802.11p VANET broadcasting performance with practical vehicle distribution," *IEEE Trans. Veh. Technol.*, vol. 64, no. 10, pp. 4756–4769, Oct. 2015.

[20] G. V. Rossi and K. K. Leung, "Performance tradeoffs by power control in wireless ad-hoc networks," in *Proc. 9th Int. Wireless Commun. Mobile Comput. Conf. (IWCMC)*, Jul. 2013, pp. 1343–1347.

[21] X. Guan, R. Sengupta, H. Krishnan, and F. Bai, "A feedback-based power control algorithm design for VANET," in *Proc. Mobile Netw. Veh. Environ.*, 2007, pp. 67–72.

[22] J. Tian and C. Lv, "Connectivity based transmit power control in VANET," in *Proc. 8th Int. Wireless Commun. Mobile Comput. Conf. (IWCMC)*, Aug. 2012, pp. 505–509.

[23] S. Sharafkandi, G. Bansal, J. B. Kenney, and D. H. C. Du, "Using EDCA to improve vehicle safety messaging," in *Proc. IEEE Veh. Netw. Conf. (VNC)*, Nov. 2012, pp. 70–77.

[24] K. Bilstrup, E. Uhlemann, E. G. Strom, and U. Bilstrup, "Evaluation of the IEEE 802.11p MAC method for vehicle-to-vehicle communication," in *Proc. IEEE 68th Veh. Technol. Conf. (VTC-Fall)*, Sep. 2008, pp. 1–5.

[25] X. Shen, R. Zhang, X. Cheng, Y. Yang, and B. Jiao, "Distributed multi-priority congestion control approach for IEEE 802.11p vehicular networks," in *Proc. 12th Int. Conf. ITS Telecommun. (ITST)*, Nov. 2012, pp. 93–97.

[26] C.-W. Hsu, C.-H. Hsu, and H.-R. Tseng, "MAC channel congestion control mechanism in IEEE 802.11p/WAVE vehicle networks," in *Proc. IEEE Veh. Technol. Conf. (VTC Fall)*, Sep. 2011, pp. 1–5.

[27] I. Koukoutsidis and V. A. Siris, "802.11e EDCA protocol parameterization: A modeling and optimization study," in *Proc. IEEE Int. Symp. World Wireless, Mobile Multimedia Netw. (WoWMoM)*, Jun. 2007, pp. 1–9.

[28] G. V. Rossi, K. K. Leung, and A. Gkelias, "Density-based optimal transmission for throughput enhancement in vehicular ad-hoc networks," in *Proc. IEEE Int. Conf. Commun. (ICC)*, Jun. 2015, pp. 6571–6576.

[29] P. Patras, A. Banchs, and P. Serrano, "A control theoretic approach for throughput optimization in IEEE 802.11e EDCA WLANs," *Mobile Netw. Appl.*, vol. 14, no. 6, p. 697, Dec. 2009.

[30] S. Wang, A. Song, J. Wei, and A. Hafid, "Maximizing saturation throughput of control channel in vehicular networks," in *Proc. 7th Int. Conf. Mobile Ad-Hoc Sensor Netw. (MSN)*, Dec. 2011, pp. 297–302.

[31] Y. Xie, I. W.-H. Ho, and L. F. Xie, "Stochastic modeling and analysis of unicast performance in 802.11p VANETs," in *Proc. 10th Int. Conf. Inf., Commun. Signal Process. (ICICS)*, Dec. 2015, pp. 1–4.

[32] I. W.-H. Ho, K. K. Leung, and J. W. Polak, "Optimal transmission probabilities in VANETs with inhomogeneous node distribution," in *Proc. IEEE 20th Int. Symp. Pers., Indoor Mobile Radio Commun.*, Sep. 2009, pp. 3025–3029.
[33] *Kolmogorov-Smirnov Test*. Accessed: Aug. 8, 2017. [Online]. Available: http://www.physics.csbsju.edu/stats/KS-test.html
[34] W. Zhang, Y. Yang, H. Qian, Y. Zhang, M. Jiao, and T. Yang, "Macroscopic traffic flow models for Shanghai," in *Proc. IEEE Int. Conf. Commun. (ICC)*, Jun. 2012, pp. 799–803.
[35] M. Gramaglia, P. Serrano, and J. A. Hernández, M. Calderon, and C. J. Bernardos, "New insights from the analysis of free flow vehicular traffic in highways," in *Proc. IEEE Int. Symp. World Wireless, Mobile Multimedia Netw. (WoWMoM)*, Jun. 2011, pp. 1–9.
[36] W. Song, M. N. Krishnan, and A. Zakhor, "Adaptive packetization for error-prone transmission over 802.11 WLANs with hidden terminals," in *Proc. IEEE Int. Workshop Multimedia Signal Process. (MMSP)*, Oct. 2009, pp. 1–6.
[37] T. Jiang, Y. Alfadhl, and K. K. Chai, "Efficient dynamic scheduling scheme between vehicles and roadside units based on IEEE 802.11p/WAVE communication standard," in *Proc. 11th Int. Conf. ITS Telecommun. (ITST)*, Aug. 2011, pp. 120–125.
[38] K. C. Lee, U. Lee, and M. Gerla, "Survey of routing protocols in vehicular ad hoc networks," in *Advances in Vehicular Ad-Hoc Networks: Developments and Challenges*. Hershey, PA, USA: IGI Global, 2010, pp. 149–170.
[39] S. Bharati and W. Zhuang, "Performance analysis of cooperative ADHOC MAC for vehicular networks," in *Proc. IEEE Global Commun. Conf. (GLOBECOM)*, Dec. 2012, pp. 5482–5487.

YU XIE received the B.Eng. degree in communication engineering from the Chongqing University of Posts and Telecommunications, China, in 2010, the M.Sc. degree in communication software and networks from Nanyang Technological University, Singapore, in 2012, and the M.Phil. degree in electronic and information engineering from The Hong Kong Polytechnic University, Hong Kong, in 2017. He is currently with the Wireless Network Solution Sales Department, Huawei Technologies Co., Ltd., as a Product Engineer. His research focuses on vehicular ad hoc network, including MAC protocols, traffic models, network performance modeling, and optimization.

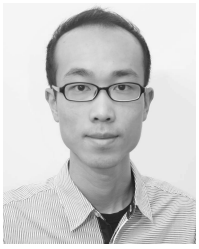

IVAN WANG-HEI HO (M'10) received the B.Eng. and M.Phil. degrees in information engineering from The Chinese University of Hong Kong, Hong Kong, in 2004 and 2006, respectively, and the Ph.D. degree in electrical and electronic engineering from Imperial College London, London, U.K., in 2010. He was with the Mobile Environmental Sensing System Across a Grid Environment Project funded by the Engineering and Physical Sciences Research Council and the Department for Transport of the U.K., and the International Technology Alliance Project funded by the U.S. Army Research Laboratory and the Ministry of Defence of U.K. during his Ph.D. studies. In 2007, he was with the IBM Thomas J. Watson Research Center, Hawthorne, NY, USA. After his Ph.D. graduation, he was with the System Engineering Initiative, Imperial College London, as a Post-Doctoral Research Associate. In 2010, he co-founded P2 Mobile Technologies Ltd., Hong Kong Science Park, and served as the Chief Research and Development Engineer. He is currently a Research Assistant Professor with the Department of Electronic and Information Engineering, The Hong Kong Polytechnic University, Hong Kong. He primarily invented the MeshRanger series wireless mesh embedded system, which won the Silver Award in Best Ubiquitous Networking at the Hong Kong ICT Awards 2012. He is an Associate Editor of the IEEE Access, and a TPC Member of IEEE conferences (ICC, WCNC, and PIMRC). His research interests are in wireless communications and networking, specifically in vehicular ad-hoc networks, intelligent transportation systems, Internet of things, and physical-layer network coding.

ELMER R. MAGSINO received the B.Sc. degree in electronics and communications engineering and the M.Sc. degree in electrical engineering from The University of the Philippines-Diliman in 2002 and 2006, respectively. He is currently pursuing the Ph.D. degree with The Hong Kong Polytechnic University, Hong Kong, focusing on data representation and dissemination in vehicular ad hoc networks. Before undertaking the academic career, he served as a Design Engineer in a power electronics company. He is also an Assistant Professor (on study leave) with the Department of Electronics and Communications Engineering, Gokongwei College of Engineering, De La Salle University-Manila, Philippines. He has also served as the Program Coordinator for the Computer Engineering program of the Department of Electronics and Communications Engineering from 2013 to 2015.